Supporting Information for

Multiscale Modelling of the Electrostatic Impact of Self-Assembled Monolayers used as Gate Dielectric Treatment in Organic Thin-Film Transistors

Alexander Mityashin[†‡], Otello Maria Roscioni[§], Luca Muccioli[§], Claudio Zannoni[§], Victor Geskin[‖], Jérôme Cornil[‖], Dimitri Janssen[†○], Soeren Steudel[†], Jan Genoe[†], and Paul Heremans[†‡].*

[†]Large Area Electronics, Imec, Kapeldreef 75, Leuven, 3001, Belgium

[‡]ESAT, Katholieke Universiteit Leuven, Kasteelpark Arenberg 10, Leuven, 3001, Belgium

[§]Department of Industrial Chemistry "Toso Montanari" & INSTM, University of Bologna, Viale del Risorgimento 4, Bologna, 40136, Italy

[‖]Laboratory for Chemistry of Novel Materials, University of Mons, Place du Parc 20, Mons, 7000, Belgium

[○]Department of Chemistry, Katholieke Universiteit Leuven, Celestijnenlaan 200F, Leuven, 3001, Belgium

* Corresponding Author

E-mail: Luca.Muccioli@unibo.it

Molecular Dynamics (MD):

Force Field

The charges and Lennard-Jones parameters for silicon and oxygen atoms in SiO_2 were borrowed from the force field by Cygan et al. [1]. Lennard-Jones parameters and bonding interactions for OTS and FDTS molecules were taken from the classic AMBER force field[2], except for the LJ parameters for fluorine atoms, for which we adopted the Mod–OPLS parameters by Song et al.[3]. Mixed interactions between silica and SAMs were evaluated with Lorentz-Berthelot rules. The torsional profiles for -Si-CH_2-, -CH_2-CH_2-, -CH_2-CF_2-, and -CF_2-CF_2- rotations were obtained by constrained wB97XD/aug-cc-pVTZ minimization carried out on the fragments $Si(OH)_3$-CH_2CH_3, CH_3CH_2-CH_2CH_3, CH_3CH_2-CF_2CF_3 and $CH_3CH_2CF_2$-CF_3, respectively (Figure S1). It is worth noting that while the torsion between a fluoroalkyl and an alkyl segment is very similar to the well-known alkyl-alkyl torsion, the torsion between two fluorinated segments is more complex, featuring three minima at about 55, 95, and 165 degrees. These torsional potentials were used to re-parameterize the corresponding terms in the molecular mechanics force field (see referfence[4] for the details of the procedure) and obtain a more realistic description of the SAMs conformation. Atomic charges for OTS and FDTS were derived from quantum-chemical calculations carried out with the program Gaussian G09[5] with DFT at the wB97XD//aug-cc-pVTZ level of theory[6] (Figure S1). In order to maximize the similarity with the chemical structure of SAMs used experimentally on SiO_2, the calculations were carried out for R-tri-hydroxyl-silanes (Figure S2).

We assumed that all tri-hydroxyl-silane groups are linked to the SiO_2 surface by single Si-O-$Si(OH)_2$-R bonds. Electro-neutrality in the system was maintained by replacing an hydroxyl group on the surface -Si-**OH** with a SAM molecule -Si-**O-Si(OH)$_2$-R** (with R alkylated or fluorinated, see figure S2), mimicking the chemical reaction between a trichlorosilane derivative and a SiO_2 substrate, followed by hydroxylation of the remaining chlorine atoms. We prepared first a fully hydroxylated surface of SiO_2 and then replaced randomly chosen surface hydroxyl groups. The "reacted" SAM oxygen atom was endowed with a LJ interaction specific to the silicon surface (the same as Si and O in the silica force field[1]), so as to promote a sort of bond formation with the surface Si atoms and to make the two atoms (O for the SAM, Si for the silica)

able to get very close, as in a siloxane bond (about 1.64 Å). This way of modeling the formation of a bond with the surface without explicitly grafting the molecules is commonly used for simulations of thiols on gold[7] and has the advantage of allowing for the self-assembly of the SAM.

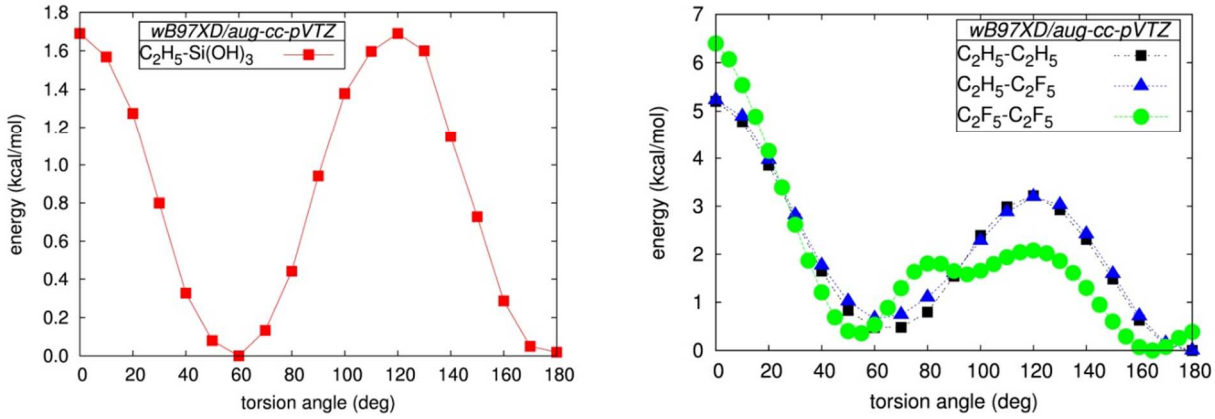

Figure S1: Torsional potentials for -Si-CH_2- (left), -CH_2-CH_2-, -CH_2-CF_2-, and -CF_2-CF_2- rotations (right) calculated at the wB97XD//aug-cc-pVTZ level.

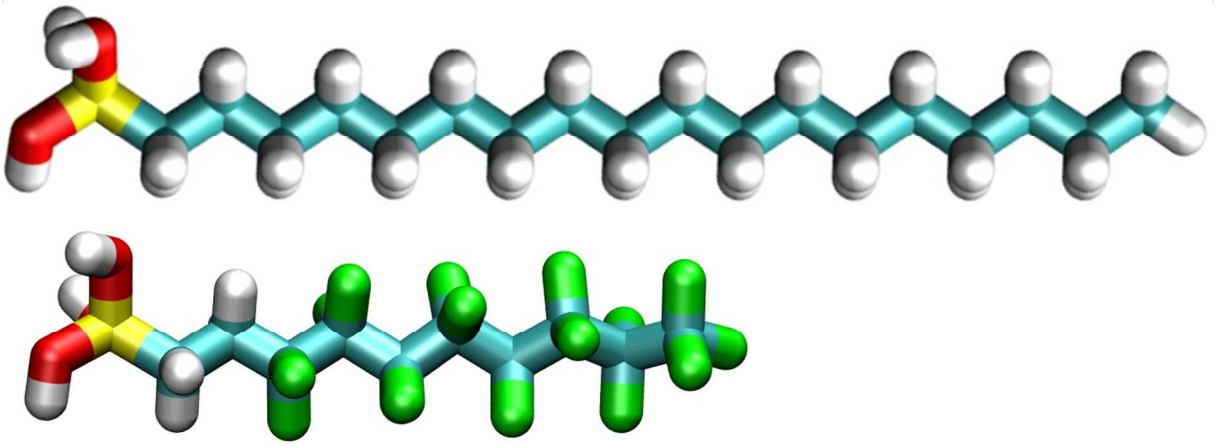

Figure S2: Equilibrium chemical structure of octadecyl tri-hydroxyl silane (OTS, top) and 1H,1H',2H,2H'-perfluorodecyl tri-hydroxyl silane (FDTS, bottom), calculated with DFT at the wB97XD//aug-cc-pVTZ level of theory.

Molecular Dynamics simulation details

An amorphous, dipole-free SiO_2 surface about 60 Å thick and with an area of 89.8x74.9 $Å^2$ was created following the procedure described in [8], followed by a simulated thermal annealing at 900 K to allow for surface reconstruction. The SAMs were modeled as a slab placed on top of the SiO_2 surface in an orthorhombic box with dimensions 89.8x74.9x200 $Å^3$. Layers of OTS and FDTS molecules were created and superimposed to the existing silicon dioxide surface, yielding coverages of 4.5 and 3.8 molecules/nm^2, respectively. These values were estimated at full coverage from the lattice vectors of OTS and FDTS in the hexagonal packing arrangement, as obtained from the first-neighbor average distances calculated from previous MD simulations of similar samples with lower surface coverage (4.2 and 3.5 molecules/nm^2, respectively). At lower coverage in fact the SAMs are not constrained to be crystalline: nevertheless we were able to observe spontaneous crystalline aggregate from which we estimated the molecular areal density at "equilibrium" for crystalline SAMs. A total of 302 molecules of OTS and 256 molecules of FDTS were used to model those SAM. MD simulations were carried out in the NVT ensemble at 300 K with the program NAMD v 2.8. Energy equilibrium was reached in about 110 ns for both samples, followed by a production time of 30 ns. Only the top 15 Å of the SiO_2 surface was let free to move, while the rest of the silica slab was kept fixed for the whole simulation.

We characterized the structure of the two SAMs in terms of orientational order, thickness and tilt angle. The orientational order was measured with the order parameter $P_2=3/2<\cos^2\beta>-1/2$, where β is the angle measuring the deviation of the orientation of the head-to-tail unit vector of each SAM molecule from the main direction of the alignment (c. f. also [4]). In the case of perfect alignment P_2 goes to one, while for a random distribution of orientations P_2 is zero. Both SAMs present a high orientational order: OTS is almost perfectly aligned ($P_2=0.97$) while FDTS is a bit more disordered ($P_2=0.86$). However, the main difference between the two structures resides in the direction of this alignment: OTS is tilted of 23 degrees with respect to the surface normal, while FDTS is on average parallel, as shown by the distribution of the tilt angle in Figure S3. The presence of the tilt for OTS is in qualitative agreement with literature data; however, for alkylsilanes, tilt angles measurement are rather scattered and cover a broad range from 10 to 40 degrees[9], so that we cannot claim a quantitative agreement. In Figure S3 we also plot the SAM density along the direction of the box perpendicular to the silica surface, which can be used to

estimate the SAM thickness. At high coverage, the experimental values are 21 ± 1 Å for OTS (reference [10], "LB-50" sample) and 13.4 ± 0.2 Å for FDTS[11]; the widths at half height of our distributions are in rather good agreement with those values. Actually, both the tilt angle and thickness are coverage-dependent and related one to another – in fact, the tilt is often estimated from the ratio between the calculated length of the SAM molecule in its extended conformation and the measured thickness. Using this argument, since the thickness measured for FDTS is 13.4 ± 0.2 Å and the calculated *ab initio* value is 13.3 Å[11], we can assume that FDTS is not tilted in real SAMs, as shown by our simulations.

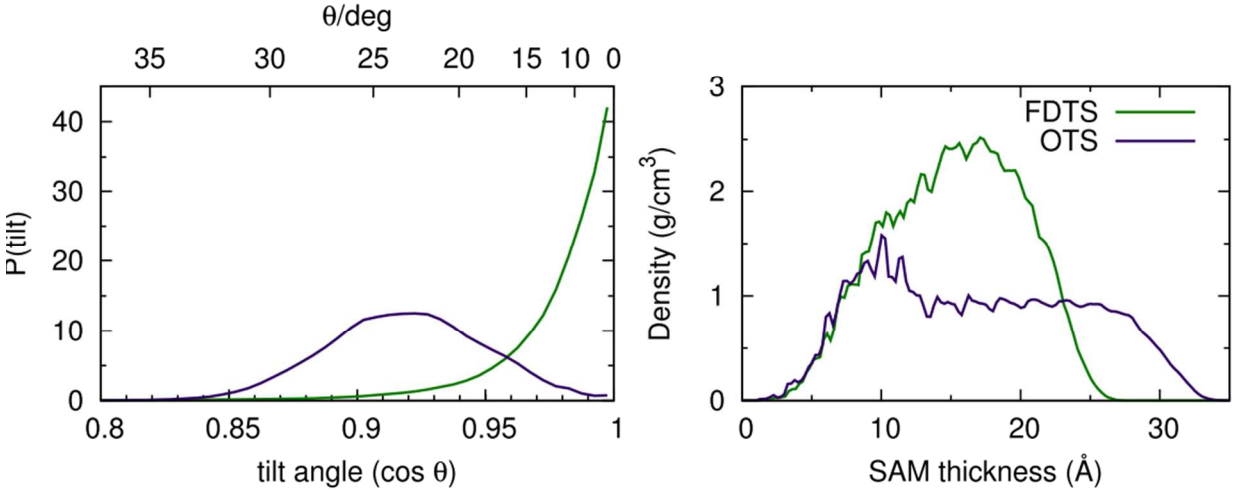

Figure S3: SAM tilt angle distribution for the head-to-tail vector (left), and mass density along the z-coordinate of the simulation box (right) for FDTS (green line) and OTS (blue line).

Device preparation: Pentacene-based OTFTs were fabricated on a doped Si/SiO_2 substrate with an aluminum back-side as a gate contact. The OTS and FDTS SAMs were vapor deposited on the substrate in standard deposition conditions (deposition temperature 140 °C, chamber pressure 8 mbar, deposition time 30-60 min, and silane solution volume 5-10 µl). Before depositing a SAM, the system is baked out at 140 °C for 30-60 minutes under vacuum to remove water and possible residues from a previous deposition. A thin film of pentacene (30 nm) is then deposited on this substrate in ultrahigh vacuum (10^{-9} Torr) by thermal evaporation in a home-built system. To ensure a comparable pentacene growth, the substrate temperature during the deposition was kept at 343 K for SiO_2 and OTS samples and at 323 K for FDTS. After the pentacene deposition,

Au top-contacts (~100 nm) are evaporated through a shadow mask to define the source and drain contacts.

Experimental measurement of surface coverage: The experimental coverage has been studied by total reflection X-ray fluorescence (TXRF) spectroscopy, a surface sensitive technique with extremely low detection limits (down to 10^{10} atoms/cm^2)[12]. Due to the insensitivity of TXRF to elements lighter than Mg, we choose to characterize a bromo undecyl trichloro silane (BUTS) SAM, containing highly "visible" Br atoms. The nature of the chemical bonding between the the trichlorosilane group and SiOx is not affected by the bromine substitution, and in general bromoalkyl SAMs have rather similar properties to other SAMs like OTS and FDTS[13–15], though of course the surface area per molecule is larger due to the bulkiness of Br. Note that although all SAMs contain detectable Si atoms, this signal cannot be efficiently used as it is easily lost in the background signal of the silicon substrate. BUTS was deposited on the SiO_2 substrate using a typical vapor deposition technique. Different pre-treatments of the SiO_2 surface were compared: O_2 plasma, UV/ozone, piranha. From the measured surface density of Br atoms, SAM coverage for different pre-treatments was calculated to be 8%, 20%, and 80% respectively (assuming a molecular area for standing BUTS of 28 A² - note even that larger values have been estimated on iron oxide[16]). The relatively high coverage of the latter sample was confirmed by high contact angle with water (<10º for SiO_2 and 90º±3º for BUTS prepared following piranha treatment). It is also worth noting that for bromine-terminated SAMs the packing density is known to be lower than for HO- or H- terminated ones[17].

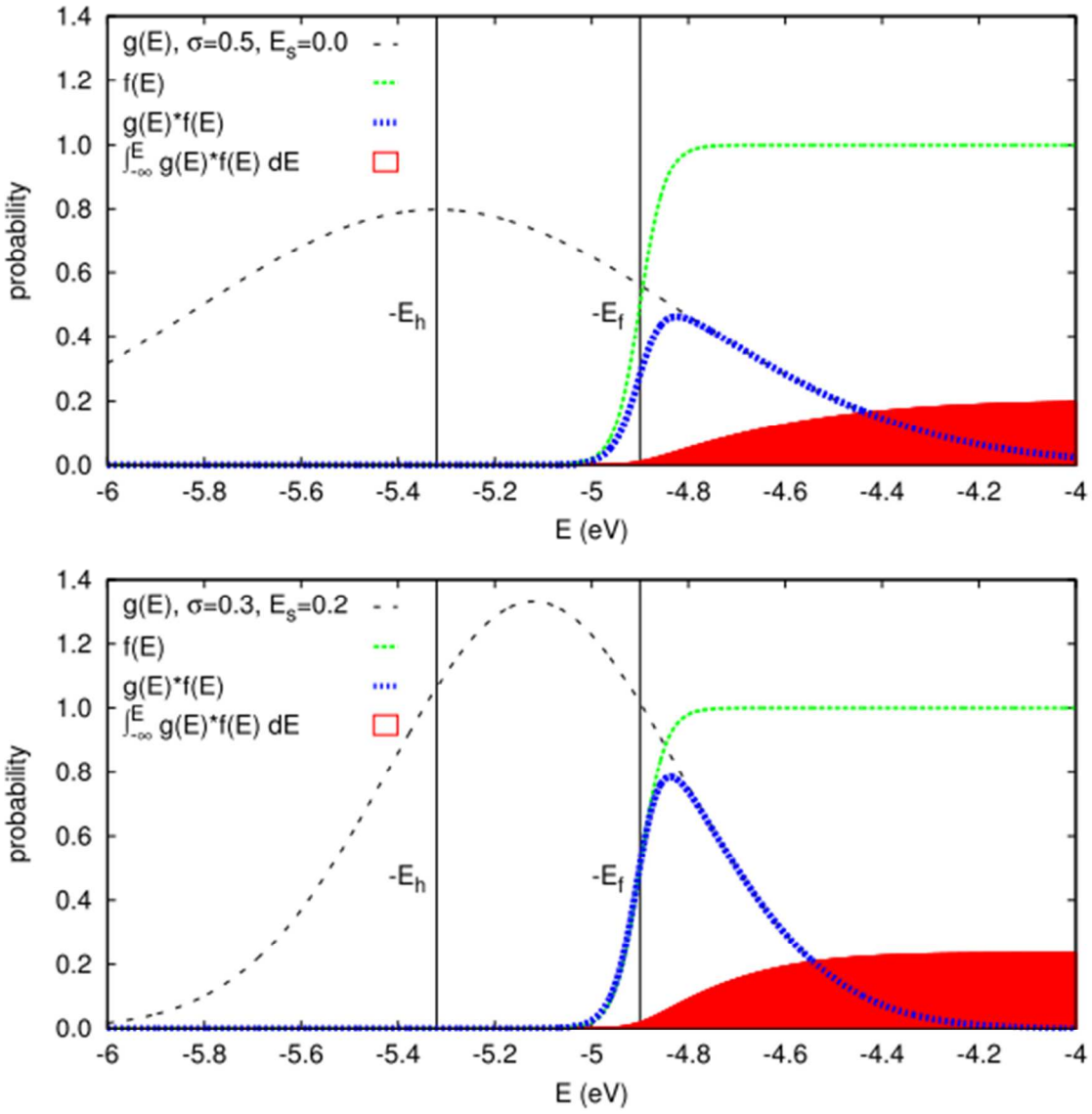

Figure S4: Illustration of the quantities modeled with equations 2-4. The density of states g(E) (Equation 2 in the main text) is a Gaussian function centered at E_s-E_h with standard deviation σ. E_h is the intrinsic hole transport level of pentacene, while E_f =4.9 eV is the Fermi level and f(E) is the Fermi-Dirac distribution function for holes (Equation 3). The interaction E_s>0 of the hole with the SAM decorated surfaces shifts the density of states towards the Fermi level, thus increasing the number N_i of carrier at the interface, given by the integral between g(E) and F(E) (Equation 4 in the main text and red area in this figure). A high roughness of the surface-hole interaction, captured by σ, also contributes to accumulating holes above the Fermi level, as shown by the comparison between the bottom and to panels.

References

(1) Cygan, R. T.; Liang, J.-J.; Kalinichev, A. G. Molecular Models of Hydroxide, Oxyhydroxide, and Clay Phases and the Development of a General Force Field. *J. Phys. Chem. B* **2004**, *108*, 1255–1266.

(2) Cornell, W. D.; Cieplak, P.; Bayly, C. I.; Gould, I. R.; Merz, K. M.; Ferguson, D. M.; Spellmeyer, D. C.; Fox, T.; Caldwell, J. W.; Kollman, P. A. A Second Generation Force Field for the Simulation of Proteins, Nucleic Acids, and Organic Molecules. *J. Am. Chem. Soc.* **1995**, *117*, 5179–5197.

(3) Song, W.; Rossky, P. J.; Maroncelli, M. Modeling Alkane+perfluoroalkane Interactions Using All-Atom Potentials: Failure of the Usual Combining Rules. *J. Chem. Phys.* **2003**, *119*, 9145.

(4) Pizzirusso, A.; Savini, M.; Muccioli, L.; Zannoni, C. An Atomistic Simulation of the Liquid-Crystalline Phases of Sexithiophene. *J. Mater. Chem.* **2011**, *21*, 125.

(5) Frisch, M. J.; Trucks, G. W.; Schlegel, H. B.; Scuseria, G. E.; Robb, M. A.; Cheeseman, J. R.; Scalmani, G.; Barone, V.; Mennucci, B.; Petersson, G. A.; Nakatsuji, H.; Caricato, M.; Li, X.; Hratchian, H. P.; Izmaylov, A. F.; Bloino, J.; Zheng, G.; Sonnenberg, J. L.; Hada, M.; Ehara, M.; Toyota, K.; Fukuda, R.; Hasegawa, J.; Ishida, M.; Nakajima, T.; Honda, Y.; Kitao, O.; Nakai, H.; Vreven, T.; Montgomery Jr, J. A.; Peralta, J. E.; Ogliaro, F.; Bearpark, M.; Heyd, J. J.; Brothers, E.; Kudin, K. N.; Staroverov, V. N.; Keith, T.; Kobayashi, R.; Normand, J.; Raghavachari, K.; Rendell, A. ; Burant, J. C.; Iyengar, S. S.; Tomasi, J.; Cossi, M.; Rega, N.; Millam, J. M.; Klene, M.; Knox, J. E.; Cross, J. B.; Bakken, V.; Adamo, C.; Jaramillo, J.; Gomperts, R.; Stratmann, R. E.; Yazyev, O.; Austin, A. J.; Cammi, R.; Pomelli, C.; Ochterski, J. W.; Martin, R. L.; Morokuma, K.; Zakrzewski, V. G.; Voth, G. A.; Salvador, P.; Dannenberg, J. J.; Dapprich, S.; Daniels, A. D.; Farkas, O.J.; Foresman, B.; Ortiz, J. V.; Cioslowski, J.; Fox, D. J. Gaussian09 Revision B.01, 2009.

(6) Chai, J.-D.; Head-Gordon, M. Long-Range Corrected Hybrid Density Functionals with Damped Atom-Atom Dispersion Corrections. *Phys. Chem. Chem. Phys.* **2008**, *10*, 6615–6620.

(7) Ahn, Y.; Saha, J. K.; Schatz, G. C.; Jang, J. Molecular Dynamics Study of the Formation of a Self-Assembled Monolayer on Gold. *J. Phys. Chem. C* **2011**, *115*, 10668–10674.

(8) Roscioni, O. M.; Muccioli, L.; Della Valle, R. G.; Pizzirusso, A.; Ricci, M.; Zannoni, C. Predicting the Anchoring of Liquid Crystals at a Solid Surface: 5-Cyanobiphenyl on Cristobalite and Glassy Silica Surfaces of Increasing Roughness. *Langmuir* **2013**, *29*, 8950–8958.

(9) Aswal, D. K.; Lenfant, S.; Guerin, D.; Yakhmi, J. V; Vuillaume, D. Self Assembled Monolayers on Silicon for Molecular Electronics. *Anal. Chim. Acta* **2006**, *568*, 84–108.

(10) Virkar, A.; Mannsfeld, S.; Oh, J. H.; Toney, M. F.; Tan, Y. H.; Liu, G.; Scott, J. C.; Miller, R.; Bao, Z. The Role of OTS Density on Pentacene and C 60 Nucleation, Thin Film Growth, and Transistor Performance. *Adv. Funct. Mater.* **2009**, *19*, 1962–1970.

(11) Kobayashi, S.; Nishikawa, T.; Takenobu, T.; Mori, S.; Shimoda, T.; Mitani, T.; Shimotani, H.; Yoshimoto, N.; Ogawa, S.; Iwasa, Y. Control of Carrier Density by Self-Assembled Monolayers in Organic Field-Effect Transistors. *Nat. Mater.* **2004**, *3*, 317–322.

(12) Klockenkämper, R.; von Bohlen, A. Total-Reflection X-Ray Fluorescence Moving towards Nanoanalysis: A Survey. *Spectrochim. Acta Part B At. Spectrosc.* **2001**, *56*, 2005–2018.

(13) Wasserman, S. R.; Tao, Y. T.; Whitesides, G. M. Structure and Reactivity of Alkylsiloxane Monolayers Formed by Reaction of Alkyltrichlorosilanes on Silicon Substrates. *Langmuir* **1989**, *5*, 1074–1087.

(14) Heise, A.; Stamm, M.; Rauscher, M.; Duschner, H.; Menzel, H. Mixed Silane Self Assembled Monolayers and Their in Situ Modification. *Thin Solid Films* **1998**, *327-329*, 199–203.

(15) Faucheux, N.; Schweiss, R.; Lützow, K.; Werner, C.; Groth, T. Self-Assembled Monolayers with Different Terminating Groups as Model Substrates for Cell Adhesion Studies. *Biomaterials* **2004**, *25*, 2721–2730.

(16) Zhang, S.; Maidenberg, Y.; Luo, K.; Koberstein, J. T. Adjusting the Surface Areal Density of Click-Reactive Azide Groups by Kinetic Control of the Azide Substitution Reaction on Bromine-Functional SAMs. *Langmuir* **2014**, *30*, 6071–6078.

(17) Cohen, Y. S.; Vilan, A.; Ron, I.; Cahen, D. Hydrolysis Improves Packing Density of Bromine-Terminated Alkyl-Chain, Silicon−Carbon Monolayers Linked to Silicon. *J. Phys. Chem. C* **2009**, *113*, 6174–6181.